

Response of Modular Composite Walls to Combined Thermal & Mechanical Load

P. N. Booth, A. H. Varma, Purdue University, West Lafayette, IN 47907, USA
S. R. Malushte, W. H. Johnson, Bechtel Power Corporation, Frederick, MD 21703, USA

ABSTRACT

The purpose of this paper is to compare the results of experimental and analytical evaluations for out of plane flexural response of steel-plate reinforced concrete (SC) wall systems subjected to simultaneous mechanical and thermal loads. A test program was designed to simulate the response and performance of a steam generator compartment wall subjected to a postulated accident causing about 10 psi uniform internal pressure at a temperature of 300° F applied for a duration of two hours against the interior wall. A fiber model was used to analytically predict the observed responses. The results showed that the SC walls can safely resist much higher pressure load while being subjected to the design temperature. Comparison of experimental results with those from the fiber model showed that a fiber model is capable of adequately predicting the SC wall response when subjected to combined thermal and mechanical load.

INTRODUCTION

SC modular walls are experiencing increasingly widespread use in nuclear power plant construction. This technology has proven to be beneficial in applications that place a premium on accelerated construction times. This is largely due to the fact that SC designs lend themselves well to prefabrication and modularization while eliminating formwork and most rebar. This substantially reduces field labor costs compared to conventional reinforced concrete construction, as it involves significant labor for formwork and rebar [1]. Prefabrication also reduces overall labor expenses by directing costs away from the field and into fabrication facilities that provide higher levels of quality, productivity, and automation. In addition, SC structural systems have demonstrated desirable structural properties such as high ductility during ultimate loading and ease of repair that make their use well suited for many applications [2].

The economic benefits of SC structural systems have generated increased interest into their applicability to a wide array of possible future uses, including those involving blast/missile resistant designs. The purpose of this paper is to provide experimental results and conclusions from a test program that sought to explore the viability of SC modules as nuclear power plant steam generator compartment walls. Literature survey indicates that there is ample test/analytical data on the behavior of SC walls subjected to mechanical loads, but not on combined thermal and mechanical load. Concrete tends to become “fully cracked” when subjected to high temperature gradient (i.e., concrete ceases to contribute in compression). Under such loading environment, it is vital that the steel plates continue to act as “bonded rebar” (i.e., not experience failure due to local buckling and/or shear connector) and that the section maintains sufficient resistance to through-thickness shear. Furthermore, the wall should be able to resist beyond-design-basis pressure loads without risking an imminent/brittle collapse mode. Finally, simple design/analysis tools are necessary to model the SC wall behavior subjected to simultaneous thermal and pressure load. With this in mind, a test setup (described below) and a fiber model analytical approach were devised to study and validate the SC wall application.

TEST SPECIMENS

The test program included two identical full scale 22-ft long beam specimens designed to represent the (essentially one-way) behavior of horizontal segments of a modular wall panel away from horizontal boundary conditions (see Figure 1). Each beam had a depth of 31-inches and a width of 30-inches. Two half-inch A572 Grade 50 steel skin plates were secured and spaced in parallel formation by steel channel spreaders welded to the inner plate surfaces (the steel channels are spaced every 30-inches). Steel rigging/bearing assemblies were welded to each end of the specimens to assist in handling and transportation and to act as concrete formwork at the ends of the beam (see Figure 3). Six inch long Nelson shear studs were welded to the inner steel faces and spaced on a 10-inch by 10-inch orthogonal layout. Once the steel fabrication was complete, 5,000-psi concrete was cast within the 30-inch void between the steel skin plates. After the concrete cured, the specimens were rotated such that the steel plates were oriented on the upper and lower surfaces.

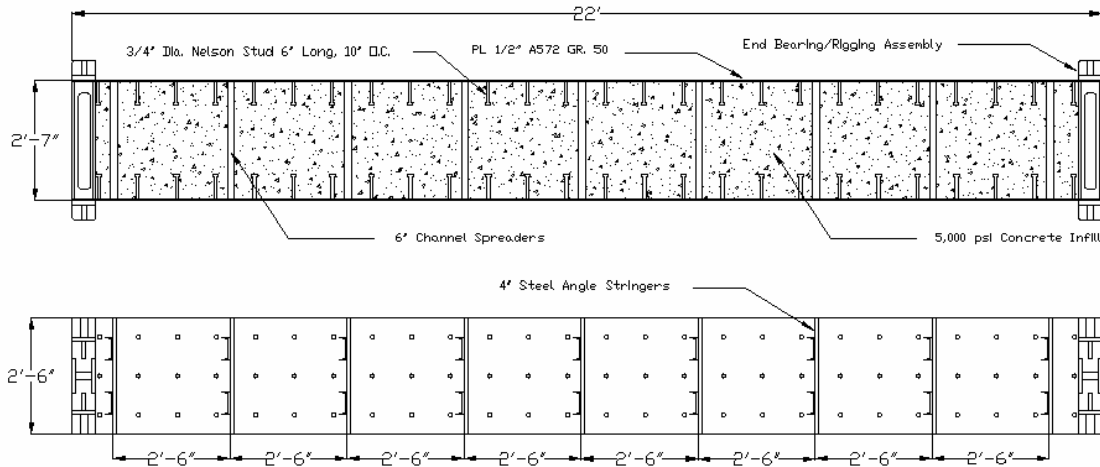


Figure 1 Elevation and Plan Views of Beam Specimens

TEST SETUP

The beam specimens were configured in a typical four point flexural test with simple supports on both ends and 100-kip capacity actuators located at 8-ft and 14-ft respectively along the 22-ft span length. The actuators were secured to a steel load frame that was bolted to the laboratory strong floor (see Figure 2). The structural loading and end conditions for both specimens were identical, but the heating (thermal loading) were different. Specimen 1 was subjected to heating in the central 6 ft. of the span, which was subjected to uniform bending moment and zero shear forces. It was used to investigate the effects of combined structural and thermal loading on the moment capacity of the SC specimens. Specimen 2 was subjected to heating in shear span, where the heating length was equal to 6 ft. and centered around one of the loading points. Specimen 2 was used to investigate the effects of combined structural and thermal loading on the shear capacity of the SC specimens.

The effects of thermal loading (heating) on the moment capacity and shear capacity of the SC specimens were investigated separately (using two specimens) because the heating equipment available for this research was limited in length (to 6 ft.) and could not heat the complete length (22 ft.) of each specimen.

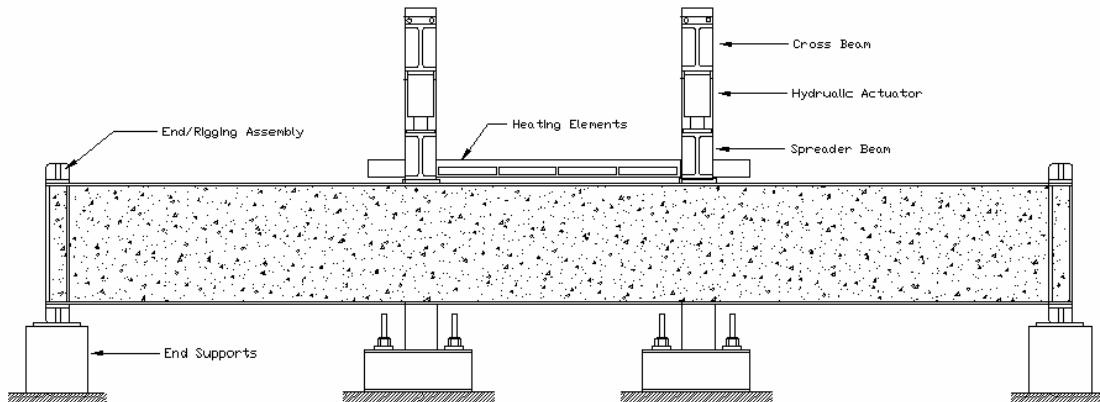


Figure 2 Sectional Elevation of Test Setup

Heating was provided by four 16-inch by 40-inch Watlow ceramic fiber radiation heaters oriented parallel to the upper steel plate creating a thermal enclosure. Figure 4 shows heating panels in place above Specimen 1. The heating panels had electrical resistance heating elements embedded in a two inch thick, rectangular ceramic fiber insulating panel. A one inch air gap was maintained between the heaters and the specimen. These heaters had sufficient power to increase the specimen surface temperature from ambient to 300°F in less than 12 minutes. For the first specimen, the heating panels were centered on the full 6 ft constant moment region at mid span and for the second specimen they were centered around one of the two load points extending 32 inches out on both sides of the actuator along the length of the beam.



Figure 3 Specimen 1 (before test)



Figure 4 Watlow heaters above Specimen 1

Four types of experimental data were recorded: vertical beam deflection, steel and concrete strains, steel and concrete temperature, and slip at the upper steel plate/concrete interface. Beam displacements were recorded along the bottom of the specimen at mid span, the two load points and one point within the shear span. Measurements of steel strain and concrete strain were recorded on the upper and lower steel surfaces and on the concrete side walls. Temperatures were measured along the concrete side wall to determine the transient experimental temperature gradient through the depth of the section and on the upper steel plate to regulate the temperatures of the heating elements.

TEST PROCEDURE

Both load tests were designed to simulate a postulated power plant high energy line break accident. In such an event, steam at an elevated temperature of 300°F and pressure of 10-psi would hypothetically be released causing compartment pressurization. For the experiment, the mechanical load was applied to the beam in the form of two equivalent transverse line loads at approximate third points along the span. It was noted that the beam's self weight caused an equivalent of 2.75-psi pressure loading. For the two hour design duration, the load was held constant at 25-kips to generate an equivalent bending moment in the constant moment region equal to that caused by a uniform pressure of about 12-psi acting over the entire top surface of the beam.

After the two hour heating phase was complete, the mechanical loads were increased until the safe working limit of the reaction frames was reached at 90-kips per actuator. This loading caused bending moment and shear forces corresponding to a pressure loading of about 36-psi; which is more than three-and-a-half times the 10-psi design load. Ability to handle such load at high temperature would demonstrate safe beyond-design-basis capacity of the specimen, and hence the modular SC walls.

RESULTS AND DISCUSSION

Both specimens had concrete shrinkage cracking that was apparent prior to testing. A visible horizontal (longitudinal) crack extending essentially the entire length of the beam was apparent on both specimens (see Figure 5). This type of shrinkage crack was an expected consequence of the plain concrete core. In addition, vertical cracks were common at locations along the beam side walls, generally at locations directly adjacent to where the internal spreader bars were located. These cracks were caused by the abrupt reduction of concrete area at cross sections containing spreaders. Two spreaders made from 6 inch channels took up 44% of the cross section at these locations.

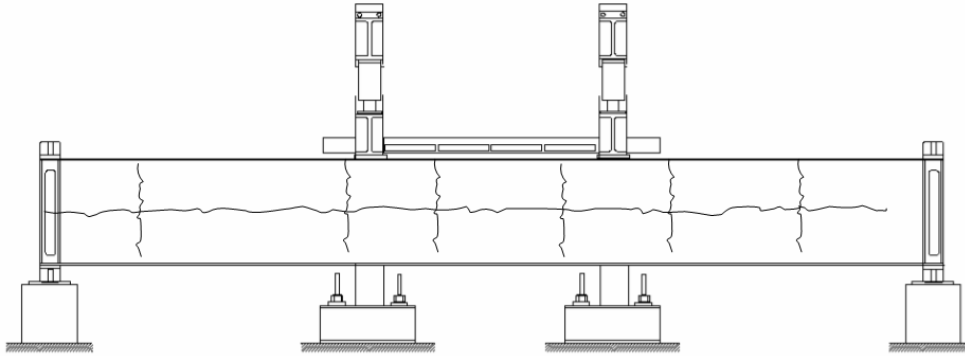


Figure 5 Shrinkage Crack Pattern before Heating

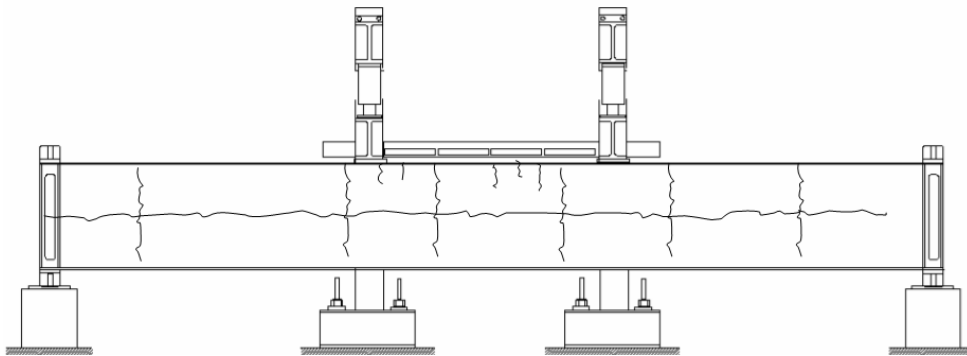


Figure 6 Addition of (small) Thermal Cracks after Heating

During the initial 25 kip load, essentially no structural concrete cracking occurred. During the heating phase, numerous cracks appeared extending down from the top of the specimen. These small cracks were typically 10 inches in length. These cracks released moisture as heating progressed. These temperature gradient induced cracks occurred exclusively along the 6 ft heated region of the specimen (see Figure 6). The final mechanical loading phase saw the addition of very few cracks outside of a few occasional flexural tension cracks extending up from the bottom of the specimen. There was no visible distress or sudden loss of strength/stiffness when the load from each actuator was increased from 25-kips to 90-kips, while maintaining the temperature at 300° F. The specimen experienced no local buckling or any shear connector failure at 90-kips load.

Fiber Model Representation of Specimen Behavior

A 2D finite element fiber model was developed for comparison to the experimental data. This model took into account the observed nonlinear thermal gradients, reduction of stiffness due to concrete cracking, and the coupled interaction between thermally and mechanically induced bending stresses. A detailed description of the fiber model can be found in Reference [8]. The fiber model employed the following assumptions:

1. Two dimensional plane stress analysis.
2. Plane sections remain plane.
3. No slip at the concrete/steel plate interface.
4. Concrete provides zero tensile strength.
5. The thermal expansion coefficient for steel is: $6.5 \times 10^{-6} / ^\circ\text{F}$ (per AISC) [3]
6. The thermal expansion coefficient for concrete is: $5.5 \times 10^{-6} / ^\circ\text{F}$ (per AISC) [3]

Steel properties were adjusted to take into account reduced strength at elevated temperatures. An elastic perfectly-plastic stress strain distribution was used. The yield strength was reduced by 10% to 45-ksi, and the elastic modulus was reduced by 0.7% in accordance with a change in temperature of (ΔT) 230° F [4]. For concrete, a nonlinear concrete stress strain curve was used per Popovics [5].

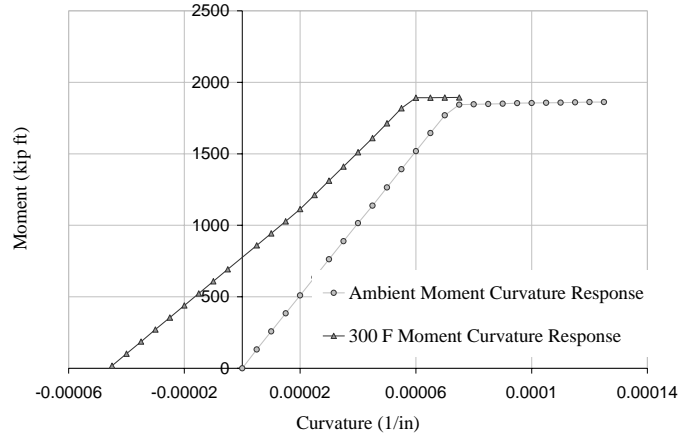


Figure 7 Moment Curvature Results for Ambient and observed temperature gradient resulting from heating top plate to 300°F

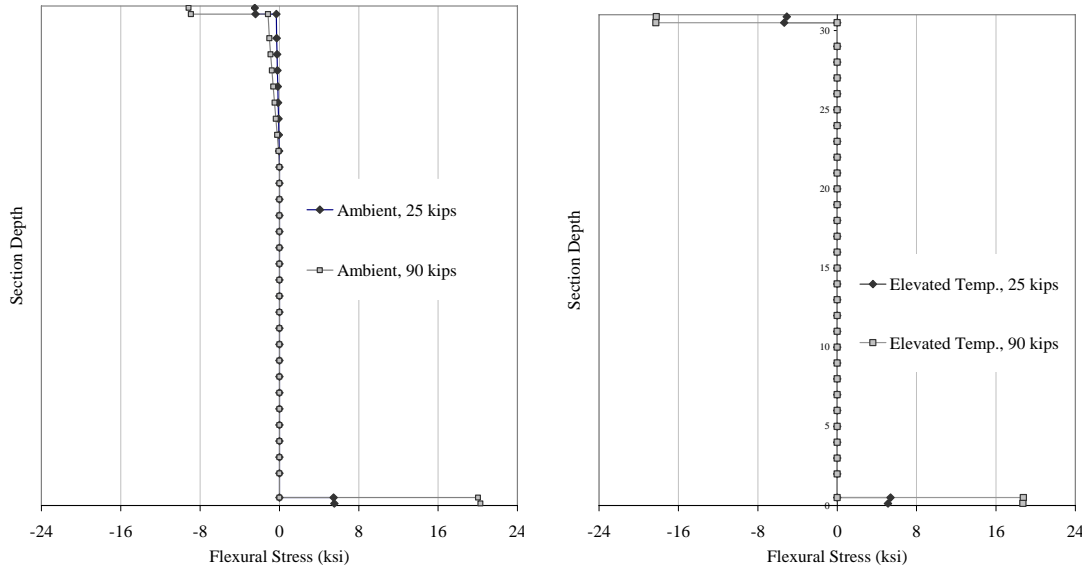


Figure 8 Fiber Model Cross Section Stresses at Ambient and Elevated Temperature

Figure 7 shows the moment-curvature ($M-\phi$) responses predicted using the fiber model. The figure includes: (i) the $M-\phi$ responses predicted for ambient conditions (no heating), and (ii) for the section subjected to thermal gradients resulting from heating the top plate to 300°F. The thermal gradients for (ii) were based on those measured for the specimens after two hours of heating. As shown, the $M-\phi$ response for the model (ii) subjected to heating (thermal gradients) had an initial curvature offset of 4.5×10^{-5} / in. at zero moment. For applied moments less than 1,000 (kip ft), the fiber model exhibited fully cracked behavior at elevated temperatures. As moments increased above 1,000 (kip ft) the concrete fibers near the top of the section experienced crack closure and developed compressive stresses, which led to partially cracked section behavior.

Figure 8 shows the longitudinal stresses predicted for the steel and concrete fibers of the section fiber model at loads equal to 25 and 90 kips corresponding to moments equal to 200 and 720 k-ft, respectively. These plots further illustrate the partially cracked behavior at ambient conditions and fully cracked behavior at elevated temperatures. At the peak load of 90-kips, the fiber model predicts the longitudinal stresses in the steel plates equal to 18.7-ksi, which is still in the elastic range.

Table 1 shows ambient and elevated temperature mid span load/deflection values and stiffnesses for both specimens. It can be seen that at ambient conditions, the fiber model and ACI effective moment of inertia approach show agreement with the experimental response. For comparison, the stiffness based on classical transformed and cracked section is also shown and tends to slightly under predict stiffness. This is consistent with strain measurements from the beam tests that showed behavior consistent with partially cracked response. Stiffness based on fully cracked section is provided for comparison as a lower bound.

Table 1 Experimental and Theoretical Load Deflection and Stiffness Data

Ambient Mid Span Deflections at 25 kips (inches)

Specimen 1	Specimen 2	Fiber Model	ACI Effective Moment of Inertia	Transformed Cracked Section
0.0573	0.0685	0.0569	0.0633	0.0713

Mid Span Deflections after Heating at 65 kips (inches)

Specimen 1	Specimen 2	Fiber Model	Fully Cracked Section
0.165	0.192	0.176	0.221

Ambient Mid Span Stiffness (kip/in)

Specimen 1	Specimen 2	Fiber Model	ACI Effective Moment of Inertia	Transformed Cracked Section
436.3	365.0	439.4	394.9	350.6

Mid Span Stiffnesses after Heating (kip/in)

Specimen 1	Specimen 2	Fiber Model	Fully Cracked Section
393.9	338.5	369.3	294.1

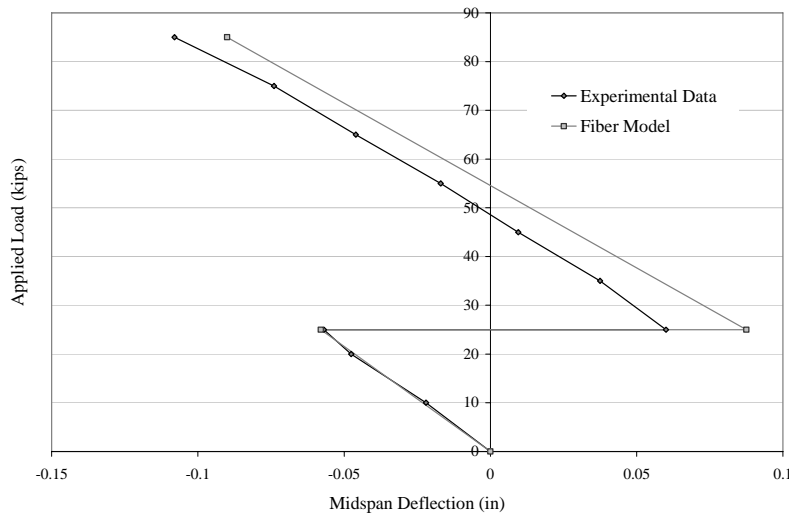


Figure 9 Experimental and Predicted Mid Span Deflections for Specimen 1.

Figure 9 illustrates further that the predicted and experimental section stiffnesses before and after heating are in agreement. Figure 9 also shows that the amount of thermally induced curvature was over-predicted by the fiber model. Accurately predicting thermal deformations proved difficult in light of uncertainties associated with comprehensive specimen temperature measurement, material thermal expansion properties, occurrence of slip and tension stiffening. The experimental temperature gradient was based on temperature measurements at 8 locations on the specimen and data from these 8 points were used to interpolate intermediate temperatures. For this reason, there is some degree of uncertainty associated with the actual internal specimen temperatures. It is noted that deflection is generally not a quantity of interest from design perspective as there are no applicable serviceability requirements for such loading. In practice, the thermal gradient is determined as an equivalent linear gradient per the procedure in the Commentary to Appendix A of ACI 349-01 [7].

CONCLUSIONS

1. Ambient flexural stiffness of SC walls can be modeled accurately using a fiber model approach or principles of fundamental reinforced concrete beam theory per ACI 318.
2. Temperature induced deformations were difficult to accurately predict because of the uncertainty associated with determining the temperature gradient and simplified modeling assumptions.
3. Exposure to elevated temperatures caused concrete cracking, leading to an expected “fully cracked” behavior, with a commensurate reduction of flexural stiffness (this observation is consistent with similar expected behavior for a conventionally reinforced cross-section). The tests indicated a reduction in flexural rigidity by 14 percent; this was found to be consistent with predictions from use of fiber model as well as based on the stiffness of steel-only section (as opposed to the stiffness of the transformed composite section).
4. The specimens resisted moments and shears for pressures as high as 36-psi, which is three-and-a-half times the expected design pressure of 10-psi. No visible distress/abrupt stiffness reduction, shear connector failure, local buckling of steel plate, loss in through-thickness shear strength, etc was noticed at these loads, thus indicating further reserve margins.

Based on the test results and analytical results, it is concluded that SC walls can be safely used for applications involving simultaneous thermal and mechanical loads, and that a simple fiber model can be satisfactorily used for design/analysis purposes.

ACKNOWLEDGEMENTS

The authors would like to acknowledge the financial and construction support provided by Bechtel Corporation, funded through its internal technical grant program. Dr. Malushte and Dr. Johnson served as the Bechtel investigators for this study. American Tank & Fabricating Company donated the two test specimens described in this study; this support is gratefully acknowledged.

REFERENCES

1. MPR-2610 Revision 2, “Application of Advanced Construction Technologies to New Nuclear Power Plants”, (Department of Energy Report), September 2004.
2. Adams, P. F., Zimmerman, T. J. E., “Design and Behaviour of Composite Ice-Resisting Walls”, “Steel/Concrete Composite Structural Systems,” C-FER Publication No. 1, Proceedings of a special symposium held in conjunction with POAC '87, Fairbanks, Alaska, 9th International Conference on Port and Ocean Engineering under Arctic Conditions, 1987.
3. Manual of Steel Construction Load and Resistance Factor Design, 3rd Edition, American Institute of Steel Construction Inc., 2001.
4. Poh, K. W., “Stress-Strain-Temperature Relationship for Structural Steel”, Journal of Materials in Civil Engineering, September/October, 2001.
5. Popovics, S., Mechanical Behavior of Materials, Proceedings of the International Conference on Mechanical Behavior of Materials, Vol. IV., The Society of Materials Science, Japan, 1972, pp. 172 – 183.

6. Sato, J. A., Vecchio, F. J., "Thermal Gradient Effects In Reinforced Concrete Frame Structures", *ACI Structural Journal*, May-June 1990, pp. 262-275.
7. ACI 349-01 "Code Requirements for Nuclear Safety Related Concrete Structures", American Concrete Institute
8. Booth, P.N., Varma, A.H. (2007) "Response of Modular Composite Walls to Combined Thermal and Mechanical Load", *Final Technical Grant Report*, submitted to Bechtel Power Corporation, Frederick, MD 21703, USA